D. JĘDRZEJCZYK*, M. HAJDUGA*

EFFECT OF THE SURFACE OXIDATION ON THE HOT-DIP ZINC GALVANIZING OF CAST IRON

WPŁYW POWIERZCHNIOWEGO UTLENIANIA NA EFEKTY CYNKOWANIA OGNIOWEGO ŻELIWA

In presented work authors analyzed the high-temperature oxidation process from the point of view of its influence on effects obtained during cast iron hot-dip zinc coating. Research concerned the influence of the high-temperature oxidation, as a preliminary stage previous to coating with zinc on the change of surface layer structure as well as subsurface layer of cast iron with flake, vermicular and nodular graphite. To obtain proper results of Zn coating the special chemical etching of cast iron after oxidation is necessary. The effects were compared to these obtained during cast iron coating without preliminary thermal processing. To comparative analysis both optical and scanning microscope, RTG measurement and profile measurement gauge results were applied. As a consequence of conducted high-temperature oxidation in subsurface layer of cast iron pores have been created, that in result of coating in liquid zinc were filled with new phase and in this way the new zone with different properties was obtained. It was additionally stated that the cast iron layer enriched in zinc is considerably thicker than layers got with application of other methods. Thickness of sub-surface layer where "after-graphite" pores are filled with zinc depends directly on the kind of graphite. When the flake and vermicular/compacted graphite is observed depth of penetration reaches 120 μm, whereas in nodular cast iron it reaches only 15μm, although sometimes single voids filled with zinc are observed at 75μm depth.

Keywords: cast iron, high-temperature oxidation, hot-dip zinc coating

W prezentowanej pracy autorzy zdecydowali się spojrzeć na proces wysokotemperaturowego utleniania z punktu widzenia jego wpływu na efekty uzyskiwane podczas cynkowania ogniowego żeliwa. Badania dotyczyły wpływu wysokotemperaturowego utleniania, jako etapu poprzedzającego cynkowanie na zmiany zarówno naniesionej warstwy, jak i warstwy przypowierzchniowej żeliwa z grafitem płatkowym, wermikularnym oraz kulkowym. W celu otrzymania właściwych efektów cynkowania konieczna jest specjalna obróbka chemiczna żeliwa po utlenianiu. Otrzymane wyniki porównano do tych, jakie otrzymuje się bez wstępnej obróbki cieplnej. Do obserwacji i badań porównawczych stosowano mikroskop optyczny, skaningowy, badania RTG oraz pomiary za pomocą profilometru. W konsekwencji przeprowadzonego wysokotemperaturowego utleniania w warstwie przypowierzchniowej żeliwa powstały „po-grafitowe" pory, które w wyniku cynkowania zostały wypełnione nową fazą i w ten sposób została utworzona nowa strefa o odmiennych właściwościach. Dodatkowo stwierdzono, że warstwa żeliwa o podwyższonej zawartości cynku jest znacznie grubsza niż uzyskana za pomocą innych metod. Grubość przypowierzchniowej strefy, gdzie „po-grafitowe" pory zostały wypełnione cynkiem ściśle zależy od rodzaju grafitu. W przypadku grafitu płatkowego i wermikularnego głębokość penetracji osiągała 120 μm, podczas gdy dla grafitu kulkowego sięgała tylko 15μm, chociaż niekiedy pojedyncze pustki wypełnione cynkiem były obserwowane nawet na głębokości 75μm.

1. Introduction

Although the hot dip zinc galvanizing process has been studied for many years it still causes a lot of difficulties. Research regards mainly steel galvanizing – influence of different technological factors (bath chemical composition, bath temperature, surface state, time of operation, reaction and fluxing agent character) on the final layer quality. Meanwhile, large majority of problems regard hot deep zinc coating of cast iron. Espe-cially defects are observed not at the crude surface but just after machining (Fig. 1). It follows from negative influence of graphite that can penetrate inside the coating and decrease it tightness (density). From the other side acids used in galvanizing technology can penetrate far inside along graphite interstitial surface and it is very difficult to wash them away. Sometimes at the galvanized cast iron surface are visible products of reaction between acid used for rinsing and metallic matrix.

* UNIVERSITY OF BIELSKO-BIAŁA, 43-309 BIELSKO-BIAŁA, WILLOWA 2, POLAND

Because of the fact that high quality cast iron produced at present – ADI, cast iron with vermicular graphite [1, 2] equals or even exceeds steel or forged elements regarding mechanical properties author decided to investigate and compare different kind of cast iron.

It is well known that hot-dip zinc galvanizing belongs to the technically advanced methods of steel and cast iron protection against environment influence. Despite intensive development of this technology there is still lack of detailed research works regarding formation of coating structure and the role that graphite precipitations can play.

Differentiation of cast iron galvanizing process in industrial practice depends on many factors: element structure, chemical composition and technical conditions of the plant. The process of producing zinc coating is composed from two main stages: etching of the base surface (hydrochloric acid, hydrofluoride acid) and of growing of the zinc layer.

For analysis of the zinc-coating structure created on iron alloys the basis is the Fe-Zn phase equilibrium diagram [3, 4]. For several dozen years this diagram has undergone many changes. About 80 years ago it was proved, that in Fe-Zn diagram occurs three phases, arising as a result of the peritectic reaction: Γ – Fe_3Zn_{10}, δ – $FeZn_7$, ζ – $FeZn_{13}$ and iron solid solution in zinc – η. Next, research referred to the different forms of δ – phase existing within different temperature range (δ_1, δ) and with different morphology (δ_C – compacted, δ_P – palisade). Also $\Gamma2$ phase that is created as a result of reaction between $\Gamma1$ and δ phases was distinguished [5].
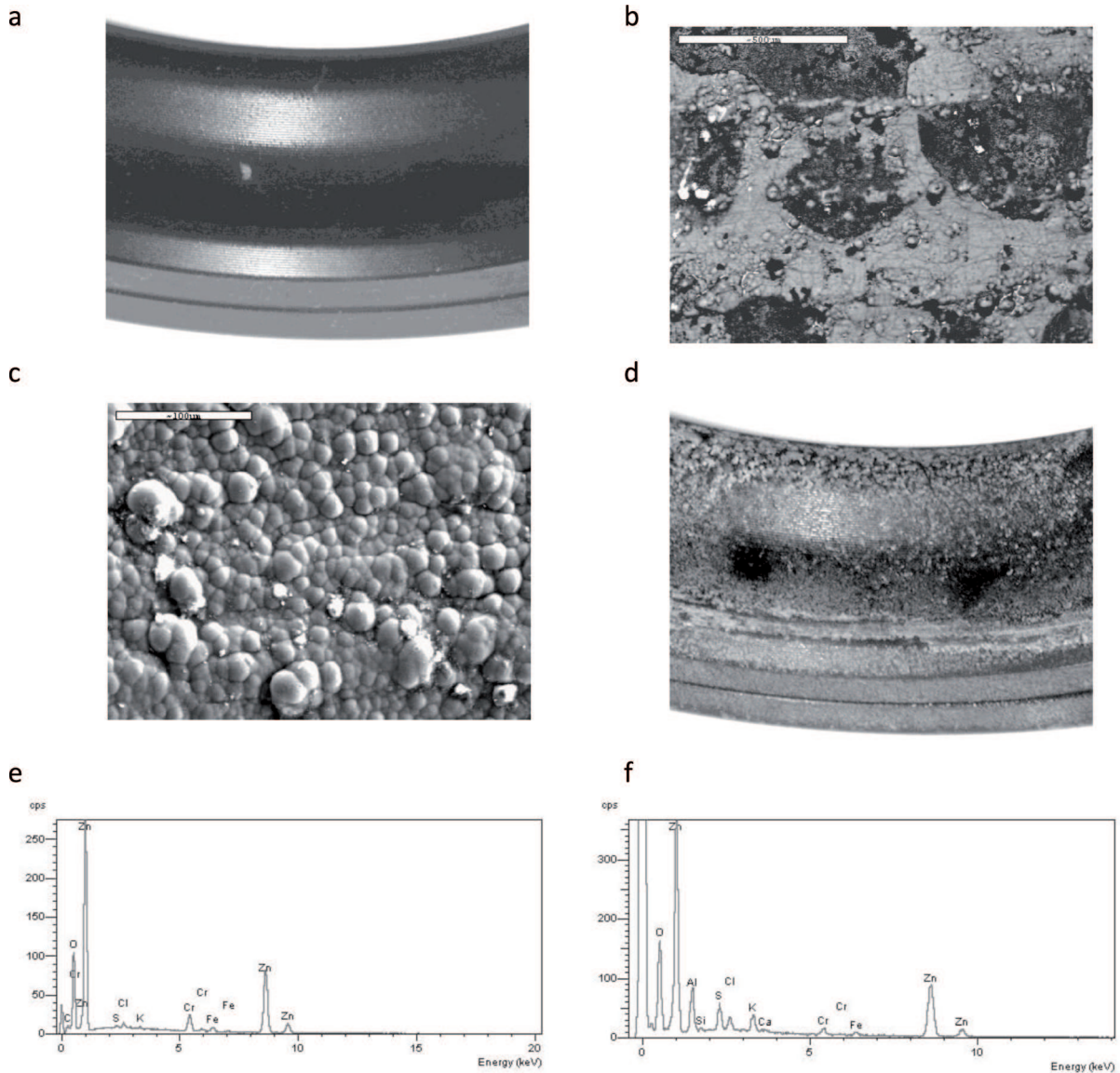

Fig. 1. Cast iron surface after zinc galvanizing – "macro" view of casting surface and surface observed under scanning microscope with EDS analysis: a, c , e – clean surface; b, d, f – impured surface [own research]

A lot of controversy regards an order of zinc coating growth. Generally accepted mechanism assumes phases formation at liquid phase boundary, from the highest content of zinc to the highest content of iron [6, 8-13] – models based on reactionary diffusion (growing of new phases with the crystal lattices different from the lattice of diffusing components). The above sequence of growing was determined in relatively long times of experiment – 1-64 hours. On the other hand in the work [15] formation of ζ phase as the first raises doubts – authors suggest that in real conditions of galvanizing that takes few minutes, a very thin layer of over-cooled liquid solution will form at the iron surface, that will support gradual creation of $\Gamma 1$ phase. The coating itself is growing as a result of peritectic reactions, thanks to it phases δ and ζ are created [5].

Structure of the zinc-coating depends also on many technological parameters, amongst which we can distinguish: the bath chemical composition, time of galvanizing or also temperature of galvanizing [7-11, 14-18].
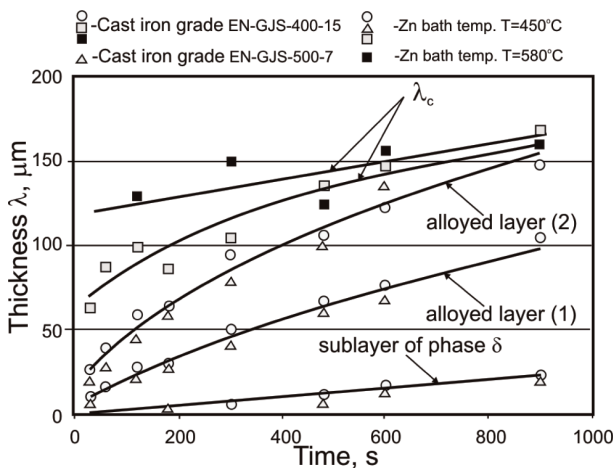

Fig. 2. Influence of the surface quality on the kinetics of zinc – coating growth at the cast iron: 1 – layer created at the crude surface of casting; 2 – layer created at the grinding surface; λ_C – total thickness of alloyed and zinc layers [19]

The machining has a significant influence on growing of zinc layer while galvanizing. At Fig. 2 a kinetics of zinc layer growth at the nodular cast iron surface is described, from which it results that surface grinding intensifies the formation process of alloyed layer with reference to the crude casting surface [19].

Additionally, a chemical composition of galvanized alloy and state of the galvanized surface influence the quality of the zinc - coating. Too high content of such elements like Si and P can essentially reduce the quality of applied coating (Sandeline effect, Sebista effect) – Fig. 3.
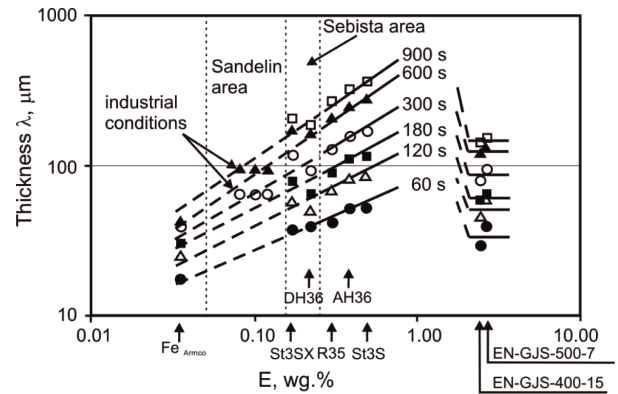

Fig. 3. Influence of the chemical composition of galvanized alloy (after mechanical treatment) on the thickness of alloyed layer; E = Si + 2.5 P, % [19]

In presented work author decided to look at the high-temperature oxidation process from the point of view of its influence on effects got during cast iron coating with Zn. The results presented in the literature usually describe the structure of cast iron scale layer or analyze the influence of different factors (the chemical composition of cast iron, shape of graphite, etc.) on oxidation mechanism. The investigation of different grades of cast iron: with flake graphite, white, nodular and ductile showed that the oxidation kinetics and the scale layer morphology depend closely on size and distribution of flake graphite. With increasing the temperature process of oxidation accelerates, the scale layer porosity enlarges and the scale layer adhesiveness to metal core gets smaller.

Although investigations have been led since many years even now some problems exist in technology that can result in differentiation of coating thickness, increasing defects number and generally decrease the surface quality. The corrosion resistance of zinc coating is determined by structure of created layer composed of few sub-layers.

The assumed investigation aims were the following: formation of the composite subsurface layer, increasing of Zn diffusion depth, formation of outside Zn layer without graphite precipitations and impurities, good quality of coating expressed by relatively low surface roughness, high corrosion resistance of created coating.

Introducing the new material into the pores' place (created as the result of high temperature oxidation in sub-surface layer of cast iron) may lead to: enlargement of thickness of subsurface cast iron layer enriched in zinc; obtaining composite surface layer with specific proprieties without necessity of expensive gear application.

Chemical composition of cast iron applied in experiment

Graphite shape	Chemical composition, wg. %						
	C	Si	Mn	P	S	Mg	Ce
Flake	3,32	1,80	0,55	0,065	0,035	0	0
Nodular	3,63	2,55	0,10	0,025	0,007	0,045	0
Vemicular	3,65	2,58	0,08	0,023	0,008	0,025	0,015

2. Experimental

During the investigations cast iron with flake, vermicular and nodular graphite melted in induction furnace of medium frequency was applied. Liquid metal was cast to sand mould with dimensions $\phi30\times300$mm (cast iron with flake and vermicular graphite) and Y2 ingots (cast iron with nodular graphite). The chemical composition of applied cast iron is presented in Table 1.

From such cast ingots samples $\phi=11$ mm and length l=110mm were turned. Then samples were put to silite furnace PKS 600/25 to oxidize. The experiment was led in five different temperatures – 850, 900, 950, 1000 and 1050°C. Samples have been taken out from the furnace separately after: 2, 4, 6, 8, 10 and 12 hours. Before oxidation and after cooling dawn samples were exactly measured, weighed, and metallographic specimens were prepared to observe surface perpendicular to sample's axis.

The scale layer was removed in two stage procedure: mechanically by sandblasting as well as chemically by dipping in solution of oxalic acid. After scale layer re-

moval the hot dip zinc coating in industrial conditions has carried out. Process consisted of the following action: degreasing – dirt and oil removal; pickling – rust, scale and carbon deposit removal; rinsing – hydrochloric acid removal; fluxing – increasing of zinc adhesion to alloy; galvanizing in temperature 445-455°C; cooling – decreasing of sample temperature.

To optical observation microscope "NEOPHOT 2" as well as "Axiovert A -100" were applied, whereas further examination was made with application of scanning microscope "Jeol J7" and X-ray analyzer "JCXA – JEOL".

Sample's surface quality was described additionally by roughness measurements made after scale layer removal – „MAHR" profile measurement gauge with "Perthometer Concept" software.

3. Analysis of results

The scale layer covering cast iron samples divides into two parts - first situated outside the initial surface of sample where porosity is directed parallel to the sample radius and second - internal layer where the direction of porosity is diverse. Additionally in subsurface layer of cast iron the area free from graphite which thickness achieves 1,6 mm is observed. So, generally the observed structure of cast iron can be divided into three layers: scale, porous subsurface zone and internal cast iron structure. The conducted process of high-temperature oxidation leads to creation not only the scale layer and subsurface porous layer but also causes the change of metal matrix character from pearlitic to ferritic.
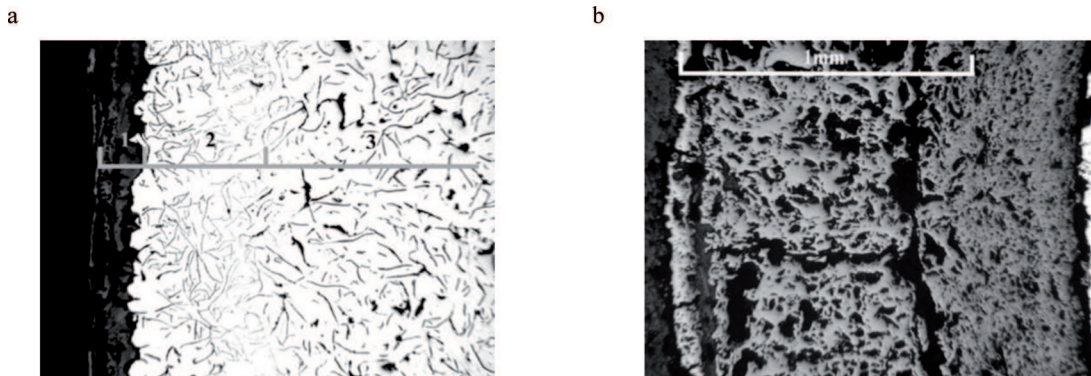

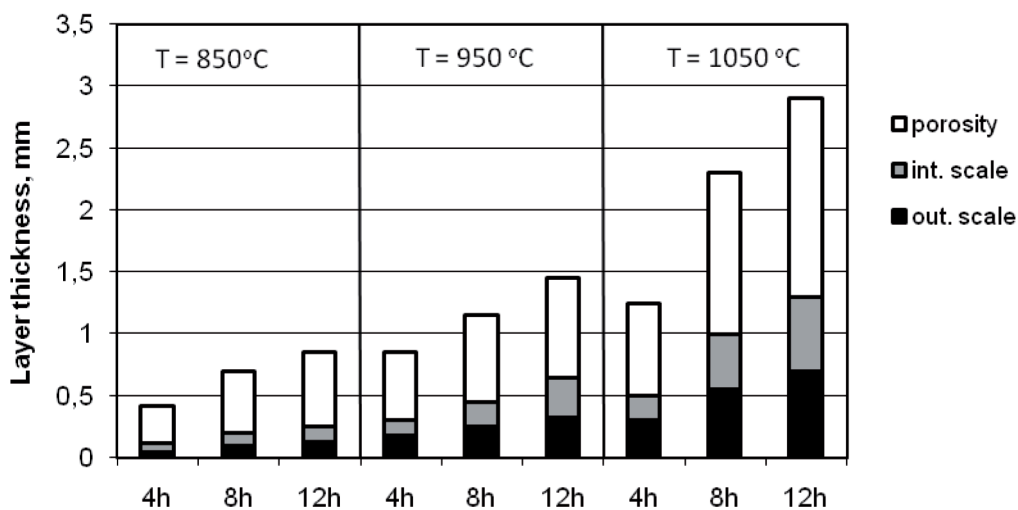Fig. 4. Zones visible in oxidized cast iron – a, and scale structure – b

Fig. 5. Depth of layers obtained in cast iron with flake graphite in dependance with temperature and time of oxidation
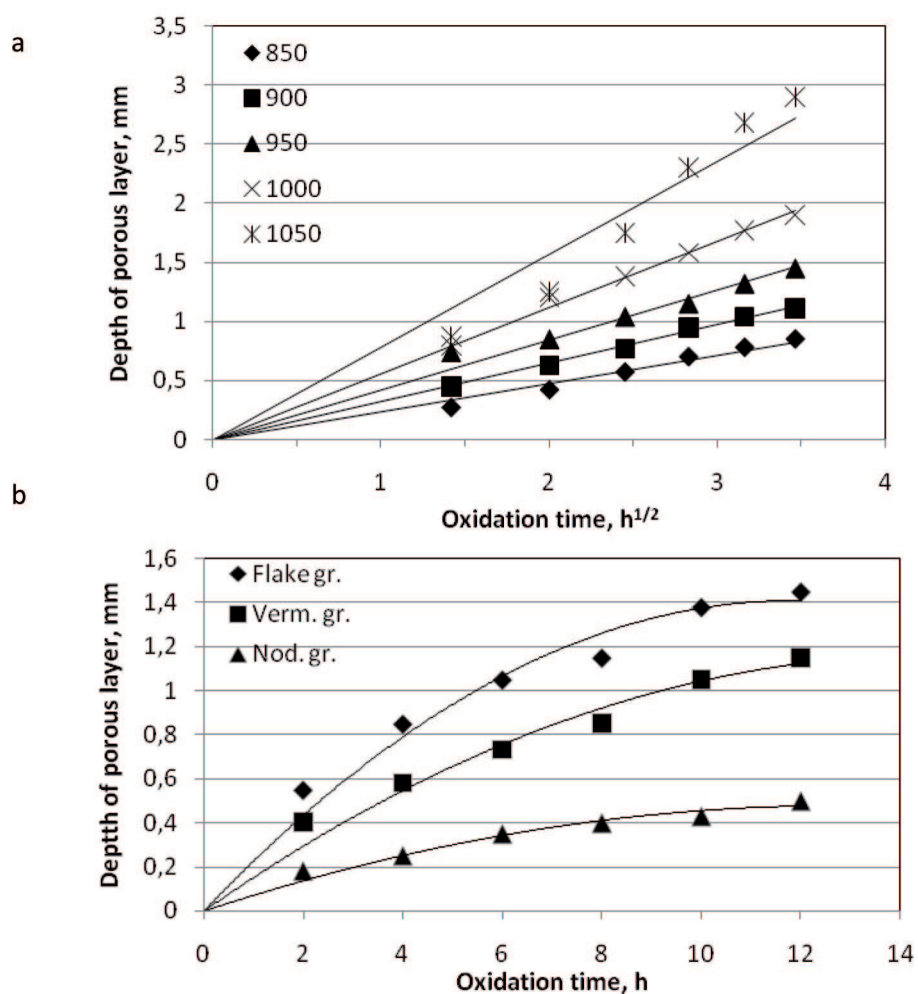

Fig. 6. Influence of different parameters on the porous layer depth: influence of temperature and time of oxidation – a (flake graphite); influence of graphite kind – b (950°C)

Both measured parameters: the diameter of metal core as well as the samples mass enlarge more intensely in initial stage of oxidation. This is probably caused by growth of scale layer, which influence can be compared to the coat inhibiting the course of oxidation process. Additionally, the silicon content interaction can't be neglected; especially in cast iron where its value is much higher than in steel. Silicon favours the decrease the speed of oxidation, both during external, as well as internal corrosion.

The influence of oxidation parameters on thickness of porous layers obtained in grey cast iron with flake graphite and influence of graphite kind is presented at Fig. 5, 6.

It follows from obtained dependence that porous layer thickness can be controlled by suitable selection of temperature and the time of oxidation as well as it depends on graphite shape existing in cast iron. Porous layer thickness decreases when graphite shape is changing from flake to vermicular and nodular.

Differentiation of the oxidation mechanism results from diverse graphite structure: flake and vermicular graphite precipitations are connected to each other, whereas nodular graphite precipitations are separated.

It can be stated that cast iron oxidation at high temperature leads to similar effect that is observed in case of pure iron - low carbon steel – at the surface the scale layer forms that is composed of three layers: wustite (FeO), magnetite (Fe_3O_4) and hematite (Fe_2O_3), additionally because of higher silicon content the internal scale layer is composed of wustite and fayalite mixture. Similar chemical composition is also observed inside decarburized graphite precipitations (Fig. 7). With reference to above to obtain composite subsurface layer not only removal of outside scale layer is necessary but also after graphite pores filler. The assumed effect can be obtained only by proper chemical treatment.
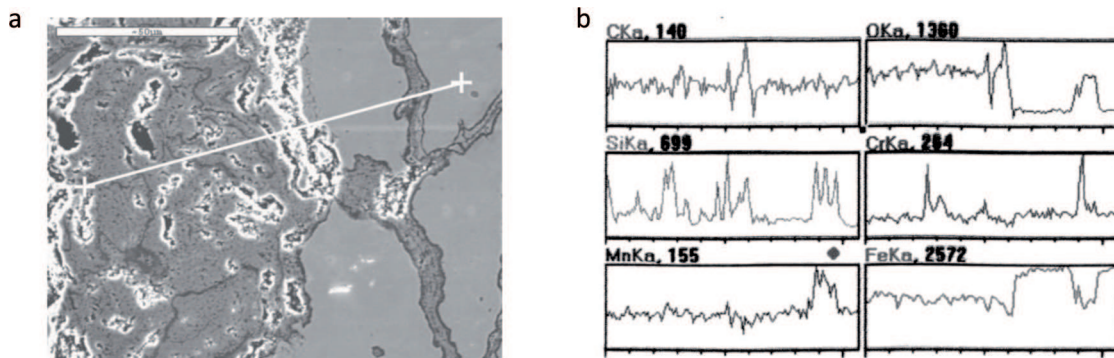

Fig. 7. Linear change of elements concentration at cross section of cast iron surface layer; a – line of measurement, b – concentration change (C, Si, Mn, O, Cr, Fe)
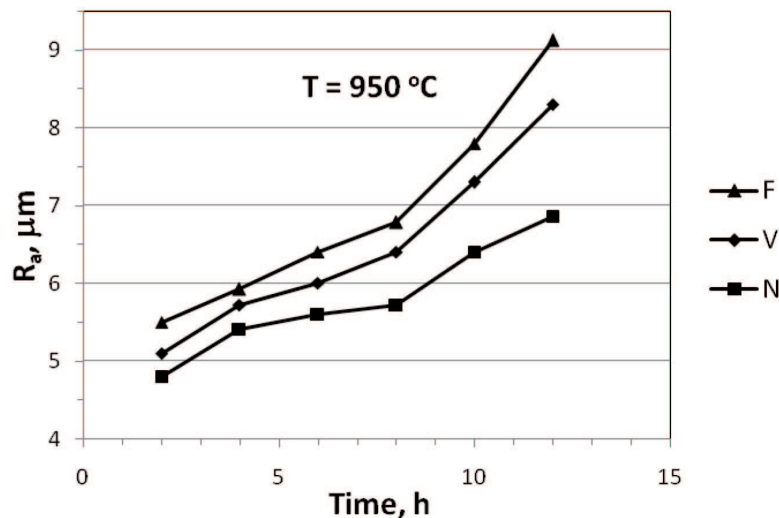

Fig. 8. Roughness R_a measured at the different kind of cast iron surface (F – flake graphite, V – vermicular, N – nodular) with dependence on time of oxidation, at temperature 950°C

It is also evident (Fig. 8, 9) that oxidation process results in higher cast iron surface roughness. Surface state is changing more rapidly in cast iron with flake graphite. In this case roughness express by R_a value can reach even more than 9 μm, after 12 hour of oxidation at 950°C. When graphite shape changes from flake to vermicular and nodular, roughness changes stay smaller. Measured roughness in vermicular and nodular cast iron after 12 hour oxidation at 950°C reaches correspondingly 8,2 and 6,8 μm.

Thickness of zinc layer that was created at the surface of cast iron samples is stable and reaches 70-100 μm. The quality of obtained surface changes in dependence on parameters of high-temperature oxidation. The greatest surface smoothness – R_a <6,3 μm was obtained for samples oxidized at parameters not higher than T⩽1050°C and t⩽8h. For example, roughness measured at sample with flake graphite, that was oxidized
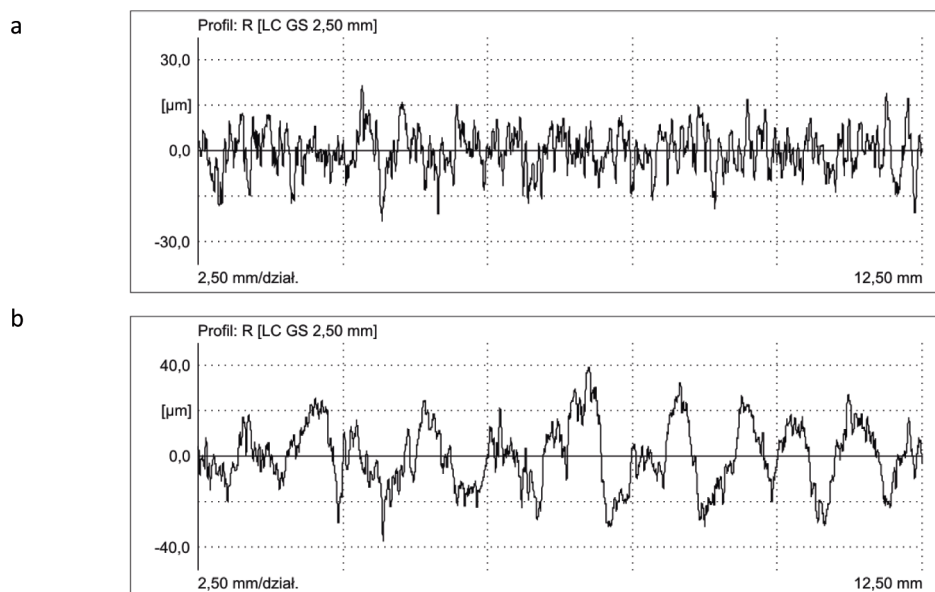

Fig. 9. An example of roughness profile measured at cast iron with flake graphite surface after oxidation at: a – T=850°C , t = 4h, R_a=5,41; b – T= 1050°C, t =12h, R_a=11,49
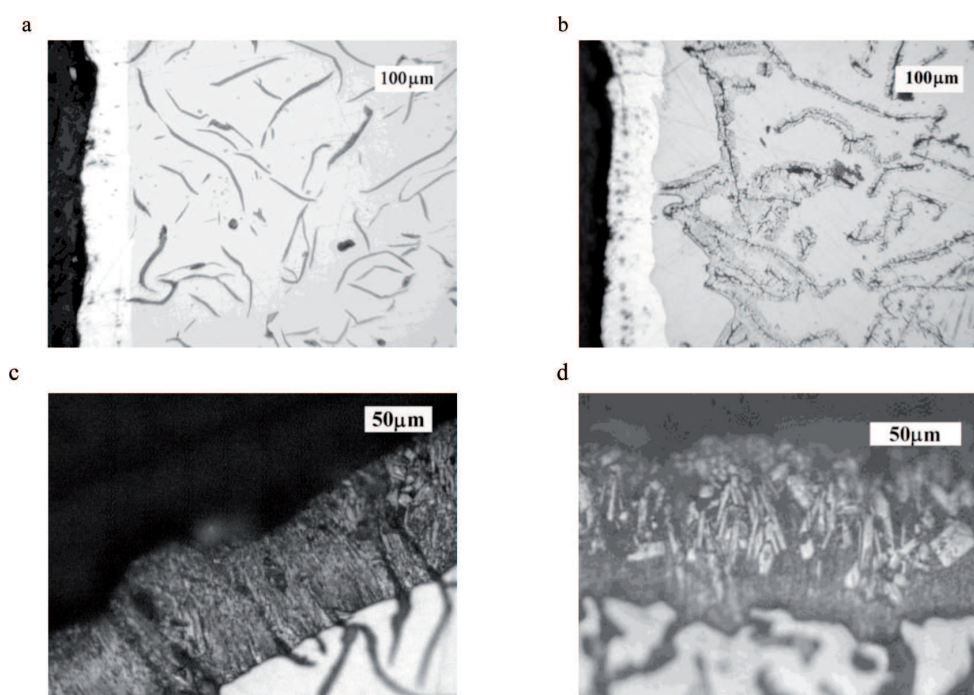

Fig. 10. Microstructure of cast iron with flake graphite after hot dip zinc galvanizing: a, c – zinc coating without oxidation; b, d – zinc coating with oxidation, 950°C, 8 hours, scale removed only mechanically

before zinc coating (T=950°C, t = 8h) gained value R_a = 3,62 μm. It means decreasing in comparison to oxidized surface after sand blasting about 3,26 μm. Although the measured values R_a don't differ essentially (R_a = 3,62 and 4,06 μm), it is visible that roughness obtaining at the surface galvanized after turning is higher than this one measured after galvanizing treatment combined with oxidation.

With reference to zinc coating of turned cast iron surface where initial roughness was in range R_a = 1,13 – 2,34 μm, as the result of zinc coating, after putting the layer with thickness about 100μm, the surface with lower quality was obtained – the roughness was in range 3,5-4,1μm – Fig. 10a.

Zinc layer observed at the cast iron surface not oxidized before has similar thickness to this one observed at the surface of oxidized samples, i.e. contained in range 70-100 μm.

Essential in this case is fact that graphite precipitations frequently penetrate in coated zinc layer and can in this way reduce its tightness (Fig. 10a, c). Such situation is not observed in case of oxidized cast iron. Cast iron, where the scale layer was removed only mechanically – using sandblasting, does not reveal deep zinc penetration inside the "after-graphite" pores – it reaches about 15μm (Fig. 10b, d).
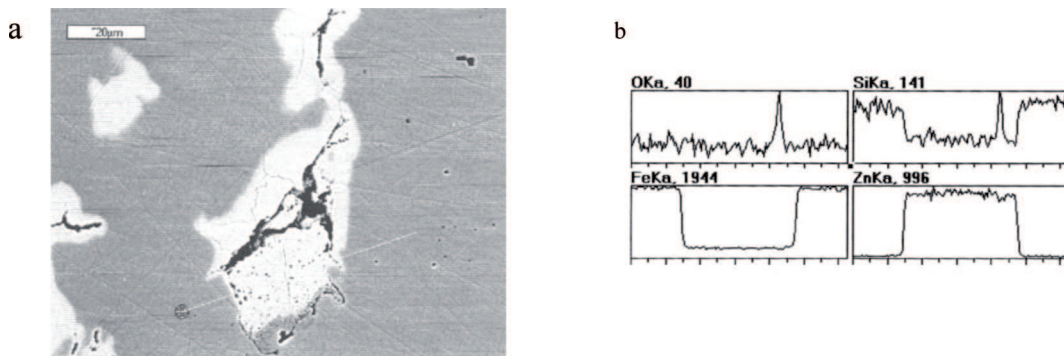

Fig. 11. Cast iron with vermicular graphite structure – a, together with linear distribution of analysed elements – b

TABLE 2

Results of X-ray point's analysis of measured elements concentrations – point's designation refers to Fig. 12b

| Element concentration, wg %										
Point No.	O	Si	Fe	Cu	Zn	Point No.	O	Si	Fe	Cu	Zn
1	0,40	0,14	4,84	0,03	94,59	11	0,33	0,04	6,98	0,00	92,65
2	0,39	0,15	5,59	0,11	93,76	12	0,26	0,14	6,60	0,29	92,71
3	0,30	0,14	6,93	0,15	92,48	13	0,39	0,00	6,29	0,03	93,28
4	0,26	1,62	96,85	0,00	1,26	14	0,40	0,02	6,58	Mn=0,05	92,95
5	0,27	1,72	97,51	0,00	0,50	15	0,34	0,03	7,08	Mn=0,08	92,47
6	0,31	1,74	97,60	0,00	0,34	16	0,26	0,10	7,81	0,00	91,84
7	0,29	1,73	97,54	0,00	0,44	17	0,41	1,81	96,42	Mn=0,05	1,31
8	0,25	1,67	97,84	0,00	0,24	18	0,34	1,81	97,44	Mn=0,03	0,37
9	0,30	1,78	97,48	0,00	0,45	19	0,32	1,92	97,42	Mn=0,20	0,13
10	0,30	0,14	9,03	0,00	90,53	20	0,30	1,99	97,43	Mn=0,28	0,00
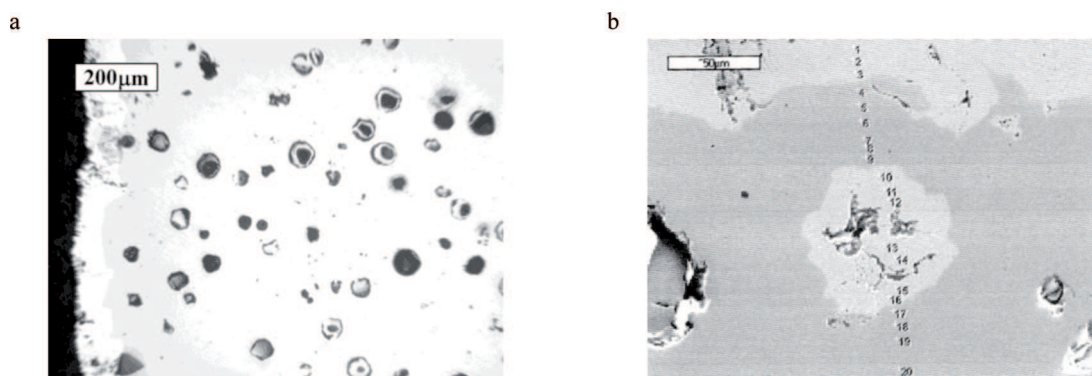
Fig. 12. Microstructure of cast iron with nodular graphite after oxidation and zinc coating with marked X-ray analysis points

Only when the chemical processing was used – dipping in solution of oxalic acid, the penetration depth considerable increases and achieves 120μm in cast iron with vermicular and flake graphite – Fig. 11.

In cast iron with nodular graphite, the depth of zinc penetration is considerable smaller, and resolves itself into filling the pores situated near the outside surface. Also in this case the filled with zinc precipitation can be observed even in distance 75μm from the surface.

The X-ray analysis made in points presented at Fig. 12b – Table 2, shows that although the zinc content between outside zinc layer and the filled "after graphite" voids, changes gradually in the range (0.24-1.26%) and near the precipitation increases imperceptibly, we cannot find that the emptiness was filled by diffusion process.

The infiltration character of "after-graphite" filling in cast iron with nodular graphite can be supported by graphite morphology – flake and vermicular graphite precipitations are connected to each other, whereas nodular graphite precipitations are separated. Occurrence of small precipitations numbers filled with zinc in nodular cast iron should be rather attributed to micro-cracks or assume that observed void is the rounded end of vermicular graphite. From the other side changes of zinc concentration between the coating and "after-graphite" filler, and also in direction from void to the core, prove intensification of zinc coating process as the result of "after-graphite" filling, that effect in widening of sub-surface layer with increased zinc concentration.

TABLE 3

Results of X-ray point's analysis of measured elements concentrations – point's designation from Fig. 13b

| Point No.	Distance from surface, μm	Element concentration, % wg.					
		C	O	Si	Mn	Fe	Zn
1	80	1,060	0,000	0,000	0,018	3,746	95,176
2	60	1,047	0,000	0,237	0,003	5,217	93,496
3	40	1,393	0,000	0,004	0,000	5,794	92,810
4	20	2,143	0,699	0,010	0,000	5,574	91,574
5	10	1,217	0,000	0,029	0,000	6,569	92,186
6	-10	0,608	0,265	1,164	0,050	97,496	0,419
7	-20	0,809	0,000	1,056	0,026	97,870	0,240
8	-40	0,372	0,000	1,324	0,041	98,204	0,058
9	-60	1,062	1,407	1,761	0,266	95,446	0,058
10	-80	0,795	1,999	0,843	0,131	96,233	0,000

a

b

c
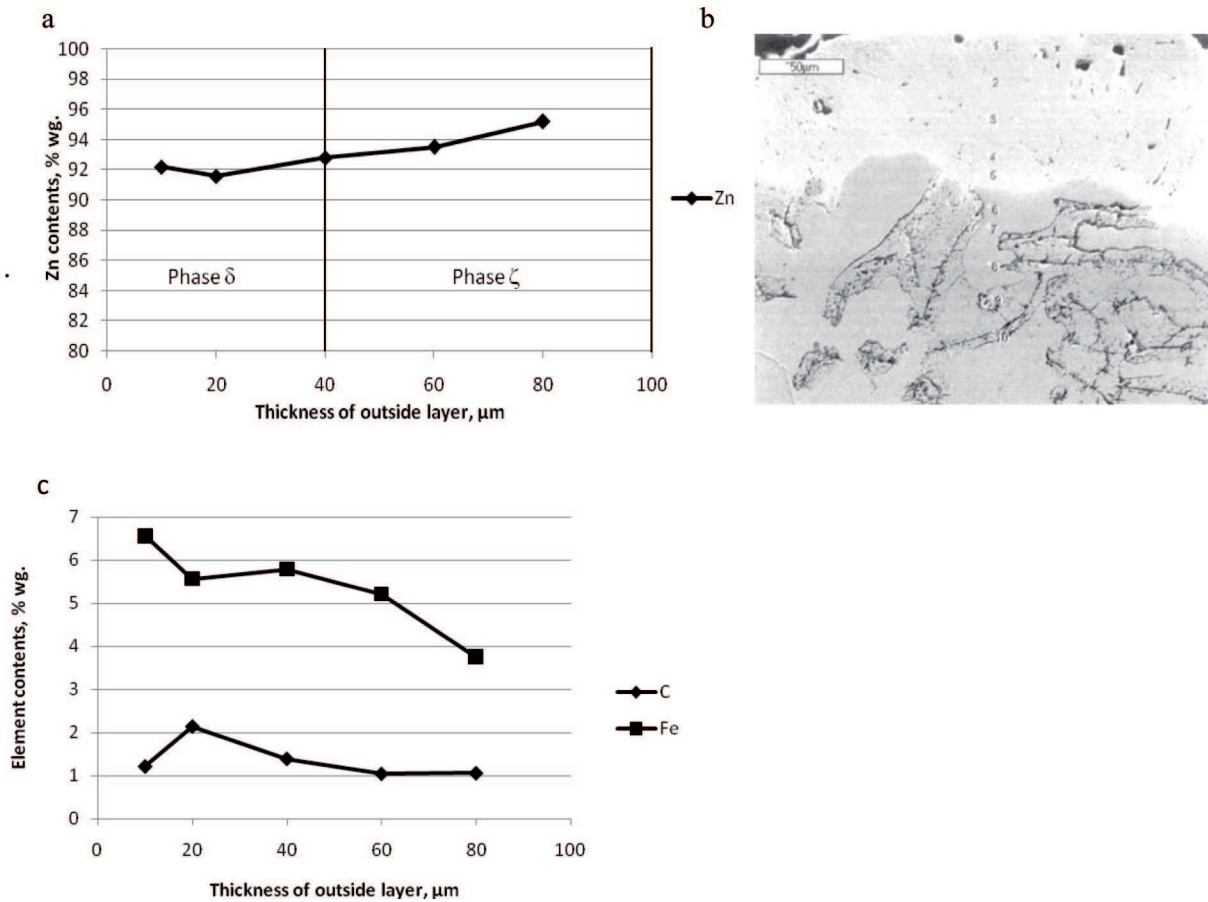
Fig. 13. The change of Zn, Fe and C concentration at the cross section of created Zn layer – a, c; points of analysis – b

Without infiltration the enlarged zinc content was measured in distance $20\mu m$ from cast iron surface. Filling of the void with zinc resulted in described case in increasing of the zone with higher zinc concentration to $75\mu m$.

The higher iron content was measured in outside zinc sub-layer, that decreases with increasing of distance from cast iron surface. Such results confirm the growth model presented in literature and at Fig. 2. It follows from measured Fe, Zn and C concentration that ζ phase thickness reaches about 60 μm whereas the rest of layer is occupied by δ phase – Table 3, Fig. 13.

Mechanism of Zn growth at cast iron surface is quite different than this one observed in Armco iron ($\Gamma 1/\delta/\zeta/\eta$) or steel case. It follows first of all from different chemical composition of alloy basis (higher silicon content and in consequence higher value of equivalent E – see Table 2 and 3) and graphite precipitations existing in the structure. From one side we can state that, in coating forming at the crude cast iron surface only small task fulfils ζ_Z phase (in comparison to coatings at the surface of steel with high value of E equivalent). From the other side, just ζ_Z phase is the dominating phase in coating growing at cast iron machined surface. At the low zinc coating time phase Γ doesn't form at all, and graphite precipitations cause irregularity of zinc coating structure.

Moreover, the RTG analysis revealed that coating surface created as the result of Zn hot-dip galvanizing of cast iron previously oxidized is free from impurities.

4. Conclusions

1. Mechanism of Zn growth at cast iron surface is quite different than this one observed in Armco iron ($\Gamma 1/\delta/\zeta/\eta$) or steel case. It results first of all from different chemical composition of alloy basis (higher silicon content and in consequence higher value of equivalent E – see Table 2 and 3) and graphite that precipitates in the structure.

2. The proposed method consisted in hot dip zinc coating of cast iron with previous high temperature oxidation makes possible creation of sub-surface layer with composite character, composed of "after – graphite" voids filled with zinc and metallic matrix, without necessity of pressure processing.

3. Because after-graphite voids are filled after oxidation with complex compound being the mixture of wustite

and fayalite, two-stage scale removal is necessary to obtain composite layer structure: mechanical – sand-blasting and chemical. The use of only mechanical processing causes, that depth of zinc penetration gets lower – to 15 μm level.

4. Thickness of sub-surface layer where "after-graphite" pores are filled with zinc depends directly on kind of graphite. When the flake and vermicular/compacted graphite is observed depth of penetration reaches 120 μm, whereas in nodular cast iron it reaches only 15μm, although sometimes single filled with zinc voids are observed at 75μm depth.

5. Roughness measured after zinc coating of cast iron being previously oxidized is sometimes even lower than roughness of zinc coating of cast iron after turning. It results first from negative influence of graphite precipitations uncovered during turning that can change locally the thickness and structure of coated layer and decrease in this way its tightness.

6. Considering the obtained results it looks very useful to verify the corrosion resistance of cast iron coated with zinc according to presented method and compare of got results with classic zinc coating effects.

REFERENCES

[1] D. M y s z k a, Archives of Metallurgy and Materials **52**, 3, 475-480 (2007).

[2] E. G u z i k, Archives of Foundry Engineering **10**, 3, 95-100 (2010).

[3] H.N. H o n g, H. S a k a, Scripta Materiala **36**, 1423-1426 (1997).

[4] H.N. H o n g, H. S a k a, Acta Metallurgica **45**, 4225-4230 (1997).

[5] D. K o p y c i n s k i, E. G u z i k, W. W o l c z y n s k i, Materials Engineering **4**, 1081-1084 (2006) (in Polish).

[6] H. O n i s h i, Y. W a k a m a t s u, H. M i u r a, Journal Japan Institute of Metals **15**, 332-337 (1974).

[7] W. W o l c z y n s k i, Monograph, Polish Academy of Science, 1-64 (2002).

[8] D. H o r s t m a n n, Stahl und Eisen **90**, 11, 571-579 (1970).

[9] D. H o r s t m a n n, F.K. P e t e r s, Stahl und Eisen **90**, 20, 1106-1114 (1970).

[10] J. M a c k o w i a k, N.R. S h o r t, International Metals Reviews **l**, 1-19 (1979).

[11] C.E. J o r d a n, A.R. M a r d e r, Journal of Materials Science **32**, 5593-5602 (1997).

[12] M. R e n n e r, Metall **35**, 865-869 (1981).

[13] J. W e s o ł o w s k i, W. G ł u c h o w s k i, L. C i u r a, Archives of Metallurgy and Materials **51**, 2, 283-288 (2006).

[14] K. K u r s k i, Cynkowanie ogniowe. Warszawa, WNT 1970.

[15] N. D r e u l l e, P. D r e u l l e, J.C. V a c h e r, Metall **34**, 834-838 (1980).

[16] J. P e l e r i n, J. H o f f m a n n, V. L e r o y, Metall **35**, 879-873 (1981).

[17] H. W o z n i c a, L. B a r y l a, Acta Metallurgica Slovaca **8**, 355-360 (2002).

[18] H. W o z n i c a, M. M i c h a l i k, Ochrona przed Korozja **11A**, 157-163 (2002).

[19] D. K o p y c i n s k i, Monograph, AGH Krakow, 2006.